WATER RESOURCES RESEARCH, VOL. 36, NO. 4, PAGES 1013–1021, APRIL 2000

Role of vegetation dynamics in enhancing the low-frequency variability of the Sahel rainfall

Guiling Wang and Elfatih A. B. Eltahir

Ralph M. Parsons Laboratory, Department of Civil and Environmental Engineering, Massachusetts Institute of Technology, Cambridge

Abstract. Rainfall observations in the Sahel region of West Africa show significant variability at the timescale of decades. Here we explore the mechanisms of this low-frequency variability using a coupled biosphere-atmosphere model which includes explicit representation of vegetation dynamics. By forcing the model with the observed sea surface temperature (SST) of the tropical Atlantic Ocean during the period 1898–1997, numerical experiments on the climate variability of West Africa have been carried out. The results of these experiments suggest that vegetation dynamics is a significant process in shaping the natural variability of the Sahel rainfall. The response of the regional climate system to large-scale forcings is significantly regulated by vegetation dynamics. The relatively slow response of vegetation to changes in the atmosphere acts to enhance the low-frequency rainfall variability. The regional climate system over West Africa has several climate regimes coexisting under the current precessional forcing. Climate transitions between different regimes act as another mechanism contributing to the low-frequency rainfall variability. Climate persistence at one regime and climate transition toward another collectively compose a distinct type of multidecadal variability.

1. Introduction

Precipitation in the Sahel region of West Africa is dominated by low-frequency variability, a characteristic not observed in the surrounding regions. While the timescale of the dominant rainfall variability is about 2–7 years for the Guinea coast region and for regions in East Africa, it is up to several decades over the Sahel region, according to analyses of observations collected during the past century [e.g., *Nicholson and Entekhabi*, 1986; *Rowell et al*., 1995]. Consistently, historical records [*Malay*, 1973, 1981; *Nicholson*, 1981; *Farmer and Wigley*, 1985] show alternate occurrence of wet and dry spells during the past several centuries, which confirms the dominance of the low-frequency variability that has been found in more recent observations in the Sahel region.

In the past three decades the extended drought in the Sahel region has motivated numerous studies on the rainfall variability over West Africa. The most important factors considered in these studies include both local factors such as land cover changes and large-scale factors such as the sea surface temperature (SST) distribution in the Atlantic Ocean and over the globe. Studies on land cover changes [e.g., *Charney et al*., 1977; *Sud and Molod*, 1988; *Xue and Shukla*, 1993; *Zhang and Henderson-Sellers*, 1996; *Zheng and Eltahir*, 1997, 1998; *Xue*, 1997] concluded that vegetation degradation reduces precipitation in the Sahel region. *Lamb* [1978a, b], *Hastenrath* [1984], *Lough* [1986], and *Zheng et al*. [1999] provided evidence that variations in the Atlantic SST influence rainfall over the Sahel region. *Folland et al*. [1991] and *Rowell et al*. [1995] investigated the impact of the regional and global SST patterns on the interannual variability of rainfall over West Africa. On the basis of statistical analysis, *Ward* [1998] associated the decadal variability of the Sahel rainfall with the variability of the north-south interhemispheric SST gradient. These studies identified the potentially important factors for rainfall variability over the Sahel region. However, the physical mechanisms behind the observed low-frequency variability are still not well understood.

Using a statistical-dynamical method, several previous studies [*Nicolis*, 1982; *Demaree and Nicolis*, 1990; *Rodriguez-Iturbe et al*., 1991; *Entekhabi et al*., 1992] suggested that the dominance of low-frequency variability in some climate records may be explained if we consider the climate system as a stochastic process driven by external forcings. Among these studies, *Demaree and Nicolis* [1990] focused on the Sahel rainfall, and viewed the low-frequency rainfall variability as a series of transitions between two stable states. On the basis of statistical analyses on rainfall data, they constructed a conceptual model using stochastic differential equations to reproduce the statistical characteristics of the rainfall time series for the Sahel region.

Recently, using a coupled biosphere-atmosphere model [*Wang and Eltahir*, 1999a] which includes the representation of complex physical processes including vegetation dynamics, *Wang and Eltahir* [1999b] (referred to as WE hereafter) demonstrated that the biosphere-atmosphere system in West Africa has multiple equilibrium states, and identified the two-way biosphere-atmosphere feedback, including vegetation dynamics, as the physical mechanism that governs the perturbation-induced transitions between different equilibria. WE then suggested that the climate fluctuations at decadal timescale can be viewed as a collective reflection of climate persistence at one equilibrium and climate transition to another. In this study, with the WE theory as the background, we further investigate the mechanisms behind the low-frequency variability of the Sahel rainfall based on long-term climate simulations using the same biosphere-atmosphere model as WE. These simulations use SST over the tropical Atlantic Ocean as the driving forcing.

Paper number 1999WR900361.
0043-1397/00/1999WR900361$09.00

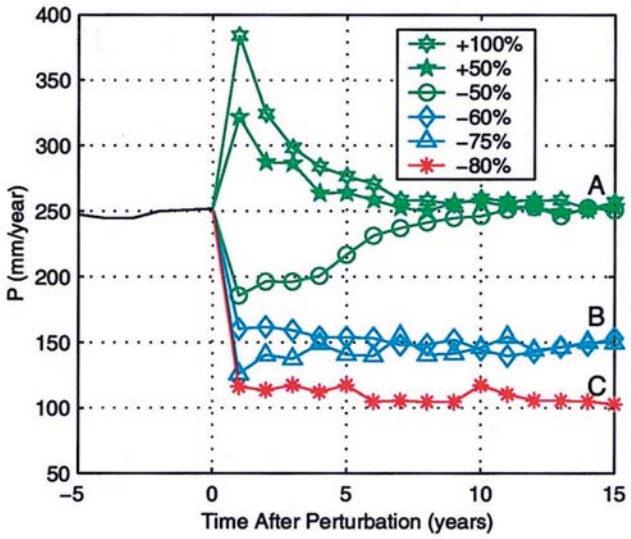

Plate 1. Response of the biosphere-atmosphere system to vegetation perturbations, using rainfall at a grid point near 16°N as an example. Vegetation perturbations take place over the grassland region (12.5°N–17.5°N) as uniform changes of grass density (as labeled in the Plate legend) and at a time when the biosphere-atmosphere system is at equilibrium.

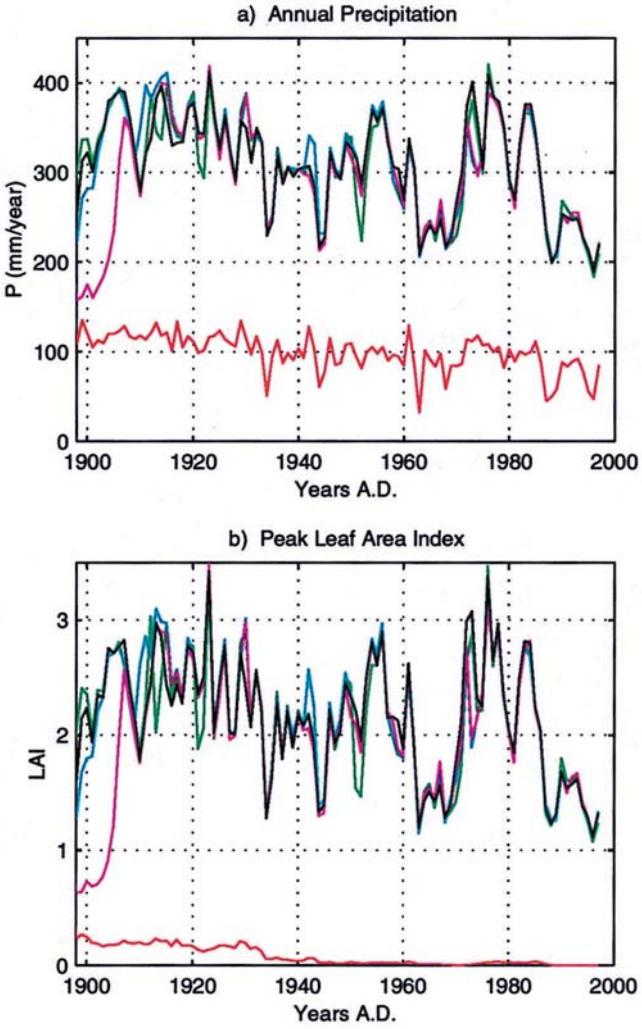

Plate 2. Time series of (a) the annual rainfall and (b) the growing season LAI at a grid point near 16°N in the control simulation Dyn-Control (black) and sensitivity experiments Dyn-Pert1 (green), Dyn-Pert2 (blue), Dyn-Pert3 (magenta), and Dyn-Oert4 (red).

2. Background

For a better understanding of the results we will present, it is necessary here to briefly introduce the background of this study, which includes the theory of multiple climate equilibria over West Africa [*Wang and Eltahir*, 1999b]. WE suggested that the response of the biosphere and the atmosphere as a coupled system to vegetation perturbations depends on the state of the postperturbation climate relative to the state of the postperturbation vegetation. Vegetation degradation causes not only a reduction in local rainfall, but also a decrease in the total water demand by the vegetation community. When the reduced rainfall is still enough for the maintenance and further growth of the postperturbation vegetation, the biosphere-atmosphere feedback is negative, which may result in either a full or a partial recovery. When the reduced rainfall is not enough to support the postperturbation vegetation, the biosphere-atmosphere feedback is positive, which enhances the initial perturbation and results in a self-perpetuating dry event. A positive feedback, or a negative one, which, however, fails to result in a full recovery, will make the system evolve into a different equilibrium state. Therefore multiple climate equilibria may exist, and the two-way biosphere-atmosphere feedback can act as a mechanism for both climate persistence at one equilibrium and climate transition between different equilibria.

The theory of WE was supported by their numerical experiments using a synchronously coupled biosphere-atmosphere model. Starting from a vegetation distribution close to today's condition in West Africa, the coupled model reached an equilibrium state which was taken as the control. By restarting the model from this control equilibrium but adding to it different levels of vegetation perturbations in the form of grass density changes over the Sahel grassland region, experiments were carried out to simulate the response of the coupled system to vegetation perturbations. As an example, Plate 1 presents the evolution of annual rainfall at a grid point near 16°N for six experiments, where the number in the plate legend stands for the magnitude of the vegetation perturbation with respect to the vegetation at the control equilibrium. Other variables (e.g., the leaf area index) describing the coupled biosphere-atmosphere system show similar evolutionary pattern. As demonstrated in Plate 1, following an increase of grass density, or a grass removal up to 50%, the biosphere-atmosphere feedback is negative, and the coupled system can fully recover from the perturbation and evolve back to the control equilibrium (curve A); with the grass removal of a larger magnitude (e.g., 60%), a positive feedback takes place which enhances the perturbation and leads the system into a second equilibrium (curve B); when the percentage of grass removal is even larger (e.g., 75%), a negative feedback occurs again, and the system evolves into equilibrium B, which signaled a partial recovery; when the perturbation magnitude further increases (e.g., 80%), a positive feedback leads to a third equilibrium (curve C), which features desert conditions at 16°N. These climate transitions are reversible: a moderate wet event can cause a transition of the coupled biosphere-atmosphere system from a

drier equilibrium to a wetter one, as shown by WE. It was then suggested that the climate persistence at one equilibrium and climate transitions between different equilibria may be responsible for the low-frequency rainfall variability in the Sahel region.

WE focused on the response of the climate system to single isolated perturbations, and assumed climatological SST distributions over the ocean. However, in reality, the regional climate system is continuously subjected to successive perturbations. Unavoidably, subsequent disturbances would modify or even override the system's response to any precedent event. For example, climate transitions from one equilibrium toward another may be interrupted or reversed by subsequent forcings. The goal of this study is to investigate how the coupled biosphere-atmosphere system in West Africa responds to successive forcings such as SST variations in the Atlantic Ocean, and to study the low-frequency rainfall variability in the Sahel region in a more realistic scenario.

3. Model Description

In this study we use the zonally symmetric, synchronously coupled biosphere-atmosphere model ZonalBAM [*Wang and Eltahir*, 1999a], which was developed for studying the two-way biosphere-atmosphere interactions over West Africa. The full model combines a zonally symmetric atmospheric model and a fully dynamic biospheric model. The atmospheric model includes the representation of atmospheric dynamics, a radiation scheme, a moist convection scheme, a boundary layer scheme, and a cloud parameterization scheme [*Wang and Eltahir*, 1999a]. The biospheric model uses the Integrated BIosphere Simulator (IBIS) [*Foley et al*., 1996], which integrates a wide range of terrestrial phenomena, including the biophysical, physiological, and ecosystem dynamical processes, into a single, physically consistent simulator. IBIS consists of four component modules: the land surface module, the vegetation phenology module, the carbon balance module, and the vegetation dynamics module. These four modules operate at different time steps depending on the processes involved. For example, the biophysical and physiological processes are simulated at the same time step as the atmospheric processes, which is of the order of minutes; the plant leaf display has a daily timescale; the carbon storage and vegetation structure are updated at an annual time step. We have modified the representation of canopy hydrological processes in the land surface module to account for the subgrid variability in rainfall interception [*Wang and Eltahir*, 1999c].

The domain of ZonalBAM spans from the southern pole to the northern pole. The land-ocean boundary is set at 6°N (which is consistent with the observed geometry of the region),

Table 1. The Vegetation Distribution in West Africa Used as the Initial Vegetation Condition for the Dyn-Control Simulation

Latitudes	Vegetation Type	Peak LAI (Plant Type)
coast to 7.2°N	rain forest	~8.5 (trees)
7.2°N–9.7°N	dry forest	~6.2 (trees)
9.7°N–12.3°N	woodland	~4.8 (trees)
12.3°N–14.8°N	tall grass	~5.2 (grass)
14.8°N–17.5°N	short grass	~1.5 (grass)
North of 17.5°N	desert	<0.02 (grass)

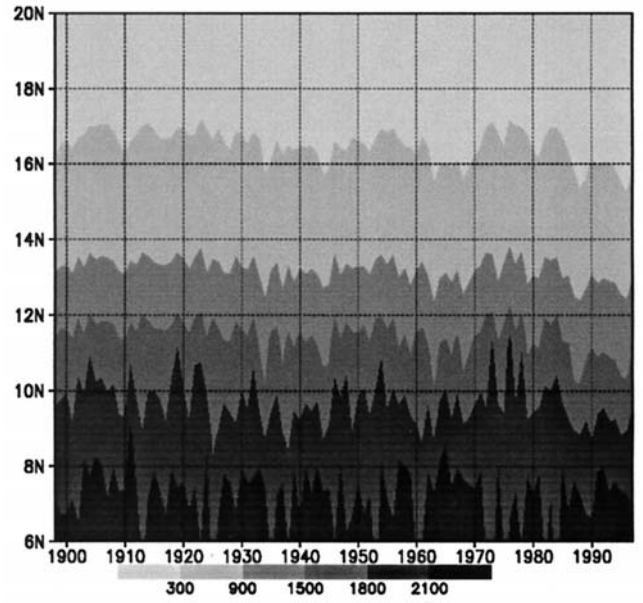

Figure 1. Rainfall distribution along latitude (y axis) and time (x axis), simulated in Dyn-Control. The unit is mm/yr.

with land in the north and ocean in the south. The horizontal resolution is close to 2.5° in the tropics, and the vertical resolution is about 40 mbar. A time step of 20 min is used. Over the ocean, SST is prescribed, but varies with time as observed. Here we interpolate in time the monthly SST observations [*Parker et al*., 1995; *Rayner et al*., 1996] averaged between 10°W and 10°E. The diurnal cycle of SST is not considered. Over land, the soil texture is fixed with time, but varies from silty loam (20% sand, 60% silt, 20% clay) near the coast to loamy sand (80% sand, 10% silt, 10% clay) in the north, according to the *Zobler* [1986] data. Vegetation is described using different plant functional types, and the vegetation canopy is divided into two layers: trees in the upper canopy and herbaceous plants in the lower canopy. Vegetation can be dynamic or static depending on the purpose of a specific experiment. Here static vegetation only means that the vegetation structure does not change from one year to the next. The diurnal cycle and seasonal cycle still exist in the plant physiological and phenological processes. When vegetation dynamics are included, the vegetation structure of each plant functional type will be updated at the yearly timescale according to the carbon budget. This results in an explicit representation of ecosystem dynamics including plant succession and competition between different plant types. Further details about the representation of ecosystem dynamics are given by *Foley et al*. [1996].

ZonalBAM has been carefully validated using observations [*Wang and Eltahir*, 1999a]. The performance of the biospheric model and the atmospheric model were tested in both an off-line mode and a synchronously coupled mode. The biospheric model was run in an off-line mode with atmospheric forcings fixed at the observed climatology to simulate the potential vegetation; the biosphere-atmosphere model was run with vegetation fixed at today's condition (i.e., vegetation dynamics is turned off) to simulate the current atmospheric climate. After these separate tests, the biosphere-atmosphere model was then run in a synchronously coupled mode with an initial vegetation distribution close to what has been observed,

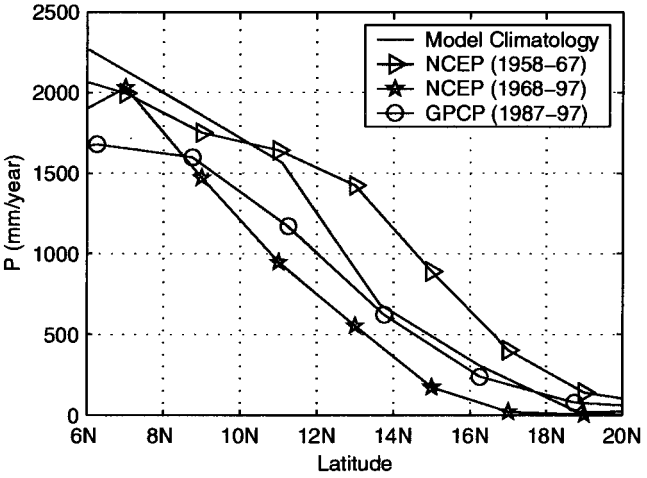

Figure 2. The model climatology (1898–1997) of the annual rainfall, compared with the climatology based on the GPCP data (1987–1997), the NCEP reanalysis data in the wet period (1958–1967), and the NCEP reanalysis data in the dry period (1968–1997). Both the NCEP reanalysis data and the GPCP data are averaged between 10°W and 10°E.

to simulate the coupled biosphere-atmosphere system. Details about the model validation are given by *Wang and Eltahir* [1999a].

4. Simulating the Decadal-Scale Rainfall Variability

4.1. Control Simulation

To study the long-term climate variability over the Sahel region, a simulation of 100 years (Dyn-Control) is carried out using ZonalBAM, with dynamic vegetation over land and SST varying from 1898 to 1997 over the ocean. In the first year of the simulation we assume that the biosphere-atmosphere system is at equilibrium A shown in Plate 1, which is an equilibrium state close to, but slightly wetter and greener than, the current climate [*Wang and Eltahir*, 1999a]. This equilibrium state was attained after running the synchronously coupled biosphere-atmosphere model for 40 years, with an initial vegetation distribution close to today's observations in West Africa and SST fixed at its climatology (1950–1979) averaged over 10°W–10°E. The meridional distribution of the vegetation type and vegetation density (represented by the leaf area index (LAI)) of this equilibrium, which is used as the initial vegetation condition of the Dyn-Control simulation, are shown in Table 1. Starting with this vegetation condition, Dyn-Control simulates the natural evolution of the synchronously coupled biosphere-atmosphere system over West Africa under the influence of the interannual variability of the Atlantic SST.

Figure 1 presents the annual rainfall distribution over West Africa from the coast to the desert during the period 1898–1997 in the Dyn-Control simulation. The rainfall climatology based on this 100-year simulation is shown in Figure 2, compared with the Global Precipitation Climatology Project (GPCP) data and the National Centers for Environmental Prediction (NCEP) reanalysis data [*Kalnay et al.*, 1996]. The GPCP data spans the period 1987–1997, amid the extended Sahel drought. The temporal coverage of the NCEP reanalysis data includes both a wet episode and the drought. For a more informative comparison, the NCEP reanalysis data are presented for the wet period (1958–1967) and the dry period (1968–1997). Over most of the land domain the model climatology falls between the observations for the dry period and the wet period. Given the assumption of zonal symmetry in the model, the comparison of the rainfall climatology between the simulation and observations is fairly good.

In Figure 1 the temporal variability of rainfall over the region north of 10°N exhibits a high degree of spatial coherency. The same statement also holds for the region south of 10°N, but with a different pattern of the rainfall temporal variability. For convenience, here we define the region 10°N–20°N as Sahel and define the region 6°N–10°N as Guinea Coast. Figures 3a and 3b present the normalized anomaly of the annual rainfall averaged over the two regions, respectively. Qualitatively, the model rainfall over the Sahel region contains more low-frequency variability than the Guinea Coast region, which is consistent with observations [*Nicholson and Palao*, 1993; *Rowell et al.*, 1995]. The following analyses focus on the Sahel region where the low-frequency rainfall variability is prominent.

Although the model captures both the rainfall climatology and the spatial contrast in the timescale of the rainfall variability, it lacks representation of several climatically important factors, which include (but are not limited to) the large-scale impact of the "Little Ice Age" that ended around 1920s [*Dansgaard et al.*, 1975; *Porter*, 1986], the anthropogenically induced land cover change since 1950s [*Gornitz and NASA*, 1985; *Fairhead and Leach*, 1998], changes in the level of CO_2 and indus-

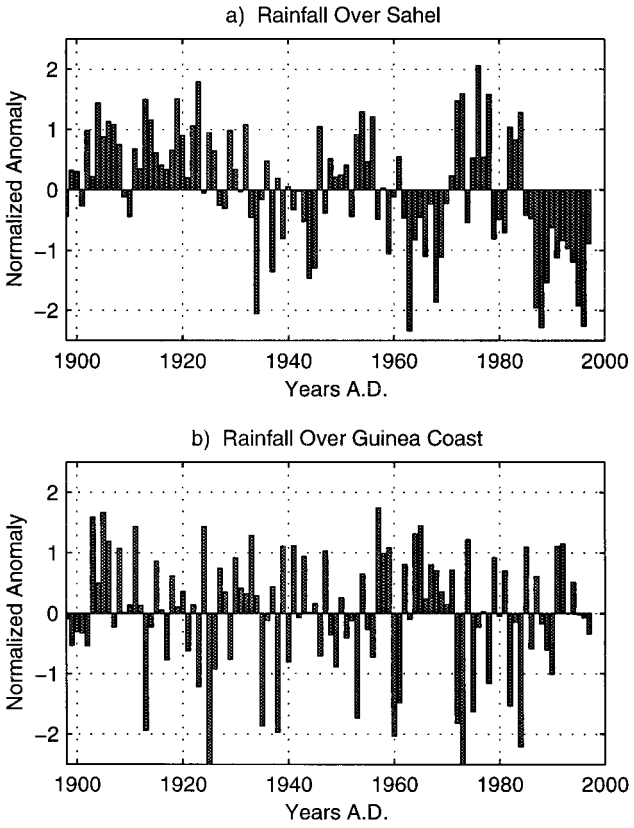

Figure 3. Time series of the normalized rainfall anomaly averaged over (a) the Sahel region and (b) the Guinea Coast region of Figure 1. The climatology for each region is based on the whole time series (1898–1997).

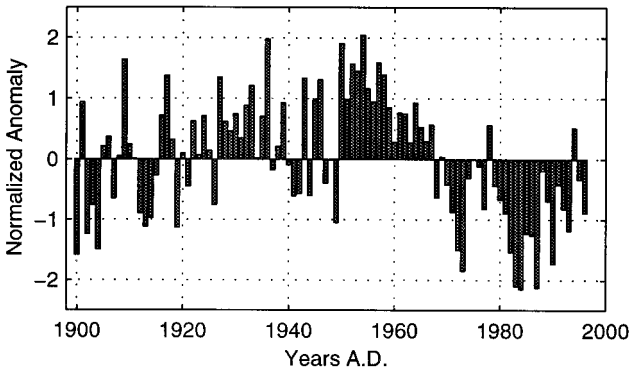

Figure 4. Time series of the normalized rainfall anomaly averaged over the region 15°W–15°E, 10°N–20°N, based on the Hulme data [*Hulme et al*., 1998]. The climatology is based on the whole time series (1900–1996).

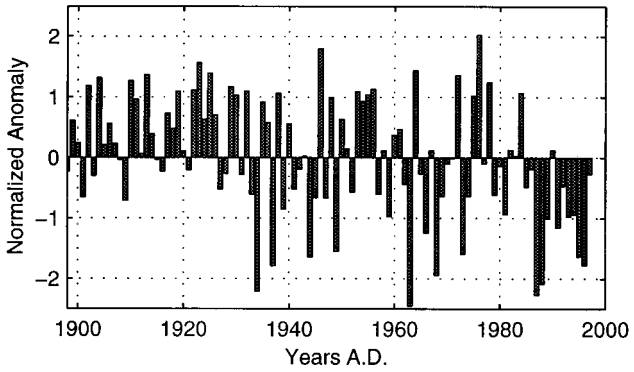

Figure 5. Time series of the normalized rainfall anomaly averaged over the Sahel region, simulated in Stat-Exp. The climatology for each region is based on the whole time series (1898–1997).

trial aerosols in the atmosphere, and the impact of global SST patterns [*Palmer*, 1986]. Another limitation of the model is the lack of synoptic disturbances and the associated interactions between the tropics and midlatitudes due to its zonally symmetric structure. Therefore, on a year-to-year basis, the model simulation may not be comparable with observations. For example, in the same scale as Figure 3a, Figure 4 presents the observed rainfall anomaly in the Sahel region for the period 1900–1996, based on the Hulme data [*Hulme et al*., 1998]. For rainfall variability at decadal timescale, two major differences between the simulation and observations are identified: the model simulates a wet episode in the first 2 decades of the century, while average to dry conditions were observed; a continuous drought was observed in the past 3 decades, while the model simulates a drought interrupted by a wet spell in 1970s. The simulated wet event early in the century is associated with the extremely low SST in the Atlantic Ocean probably related to the Little Ice Age whose broad global impact is not included in our model. At the same time, it may also have to do with the initial conditions of the simulation. As will be demonstrated in section 5, when starting with an arid condition, the model does simulate a dry episode in the beginning of the century. For the not so dry 1970s the lack of human-induced vegetation degradation may play a role.

In spite of the limitations discussed above, it is encouraging to note that the simulation captures the wet event in 1950s. In addition, the simulated wet event in 1970s, which breaks an otherwise continuous drought, takes place around a time when the severity of the observed drought was significantly alleviated (Figure 4). Most importantly, the model reproduces the low-frequency variability of the Sahel rainfall, a feature that was observed in the past several centuries and is therefore independent of most of the omitted forcings. In the following, we focus on understanding the mechanisms of this low-frequency variability.

Table 2. A List of Most of the Experiments Described in This Study

Experiment	Initial Vegetation	Vegetation Simulation	SST Forcing
Dyn-Control	as in Table 1	dynamic	as observed
Stat-Exp	as in Table 1	static	as observed
Dyn-Pert1	+25%	dynamic	as observed
Dyn-Pert2	−25%	dynamic	as observed
Dyn-Pert3	−60%	dynamic	as observed
Dyn-Pert4	−80%	dynamic	as observed
Wet2	as in Table 1	dynamic	doubled
Dry2	−80%	dynamic	doubled

In the column of "initial vegetation" the percentage describes the changes in the initial grass density over the grassland region with respect to that listed in Table 1.

4.2. Role of Vegetation Dynamics

When vegetation dynamics is included, it takes the regional climate system years or longer to recover from certain vegetation perturbations (Plate 1). This may have significant implications regarding the mechanisms of low-frequency rainfall variability. Without the functioning of vegetation dynamics a perturbation in the atmosphere would be wiped out within weeks. The corresponding timescale for soil moisture perturbations would be of the order of months. This contrast in timescales makes vegetation dynamics more important than other factors as a source for low-frequency climate variability.

An experiment Stat-Exp is carried out to study the role of vegetation dynamics in shaping the low-frequency rainfall vari-

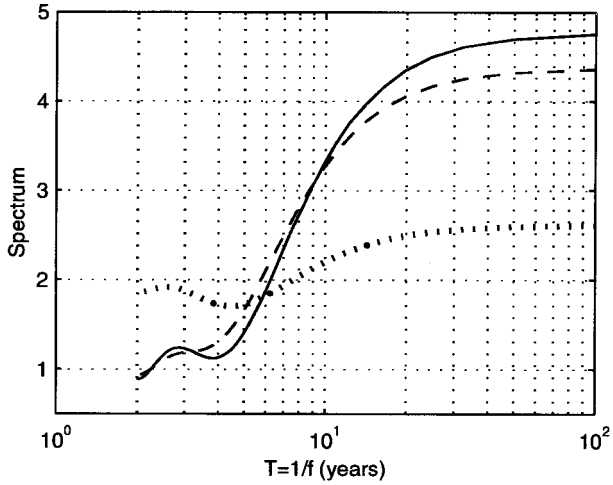

Figure 6. Spectrum of the simulated rainfall in Dyn-Control (dashed line) and Stat-Exp (dotted line), compared with the spectrum of the observed rainfall (solid line) based on the Hulme rainfall [*Hulme et al*., 1998].

ability over the Sahel region. Conditions of this experiment, together with most other experiments described in this study, are listed in Table 2 for a convenient comparison with the Dyn-Control simulation. Stat-Exp is similar to Dyn-Control but assumes static vegetation conditions; that is, vegetation distribution during the period of 1898–1997 remains fixed at the same condition as the first year of the Dyn-Control simulation. Therefore the rainfall variability simulated in Stat-Exp merely reflects the response of the atmospheric climate to SST forcings, while the rainfall variability simulated in Dyn-Control results from both SST forcings and the impact of vegetation dynamics.

In the same scale as Figure 3a, Figure 5 shows the time series of the rainfall anomaly averaged over the Sahel region based on Stat-Exp. It is readily noticeable that the annual rainfall in the Dyn-Control simulation contains significantly more low-frequency variability than the Stat-Exp simulation. As a quantitative measure, Figure 6 shows the spectrum of the Sahel annual rainfall based on the Dyn-Control (dashed line) and Stat-Exp (dotted line) simulations, compared with the spectrum based on the Hulme data (solid line). The simulation with dynamic vegetation (Dyn-Control) not only captures the dominance of low-frequency components in the rainfall variability, but also reproduces the full spectrum of the rainfall variability with reasonable accuracy. In contrast, the annual rainfall in the simulation with static vegetation (Stat-Exp) features much less low-frequency components but more high-frequency variability. Figure 6 suggests that vegetation dynamics enhances the low-frequency variability and suppresses the high-frequency variability of the Sahel rainfall. The response of the regional climate system to forcings such as the global and regional SST variations is significantly regulated by vegetation dynamics, without which the low-frequency rainfall variability over the Sahel region is unlikely to be as significant as observed.

The slow response of the vegetation to changes in the atmosphere carries the key for understanding the role of vegetation dynamics in enhancing the low-frequency rainfall variability. When the SST or any other forcing causes a significantly wetter-than-normal (drier-than-normal) event, vegetation develops denser (thinner) than normal, especially if this event spans several years. When the driving forcing ceases to operate, the biosphere-atmosphere system still has a denser-than-normal (thinner-than-normal) vegetation, which is equivalent to the situation after a vegetation perturbation. In the next several years following the termination of the original event, the biosphere-atmosphere system will be in the process of a recovery from a vegetation anomaly that favors wetter-than-normal (drier-than-normal) conditions. As a result, the original event gets amplified and extended by vegetation dynamics.

For the above described mechanism to hold, vegetation must have a "memory" long enough to carry the rainfall information from one year to the next. This is obvious over the forest region, since the forest canopy is supported by woody structures which result from the multiyear accumulation of woody biomass. Over the Sahel region which is the focus of this study, the dominant plant species is grass [*Bourliere and Hadley*, 1983]. According to *Menaut* [1983, p. 120], perennial grass is the dominant grass species in West Africa; annual grass is competitively weak and only constitutes a fleeting component of the ecosystem, "filling the gaps when the opportunity arises." Therefore, in the model we use, herbaceous plants are simulated as perennials. Although the aerial parts of the perennials die out in the dry season, their underground structures remain alive. In the beginning of the growing season, instead of starting from seeds as annuals usually do, the perennials start from the underground structure which accumulates from year to year. It is this perennating underground structure that provides the multiyear memory for the grass ecosystem.

5. Sensitivity to Initial Conditions

5.1. Multiple Climate Equilibria

The century-long simulations in section 4 start from the biosphere-atmosphere conditions at the equilibrium A in Plate 1. The assumption that the climate system in 1898 was at this specific equilibrium may not be justifiable. First, it is uncertain whether the biosphere and the atmosphere in 1898 were at equilibrium. Second, even if the biosphere-atmosphere system was anywhere close to an equilibrium, it is hard to identify that equilibrium due to the multiple-equilibrium nature of the climate system (Plate 1). To address the issue of uncertainty associated with initial conditions, we perform a group of sensitivity experiments using dynamic vegetation, each with a different degree of initial vegetation perturbation in the grassland region where the coupled biosphere-atmosphere system is highly sensitive to vegetation changes. Four experiments, Dyn-Pert1, 2, 3, and 4, will be presented in this study. With respect to the initial condition of the Dyn-Control simulation (Table 1), Dyn-Pert1 features a 25% increase of grass density, while Dyn-Pert2, 3, and 4 feature a grass removal of 25, 60, and 80%, respectively (Table 2).

Using the annual rainfall and the growing season LAI at a grid point near 16°N as examples, Plates 2a and 2b present the sensitivity of the climate system to initial conditions. The response in other parts of the perturbation zone follows a similar pattern. Despite an initial vegetation difference of +25, −25, and −60% over the grassland region in Dyn-Pert1, Dyn-Pert2, and Dyn-Pert3, respectively, simulations in these three experiments converge with the Dyn-Control simulation within several years. After the first convergence, although some local differences of small magnitudes do exist, a very good agreement between different simulations is observed. For convenience, in the following, we refer to this climate regime as the "wet regime." In Dyn-Pert4, with a grass removal of 80%, a significantly drier climate (referred as the "dry regime") results, which features desert condition at 16°N where the wet regime features short grass. Experiments with 70 and 75% grass removal (not shown here) all coverage to the dry regime. Further experiments failed to introduce a third climate regime.

The sensitivity of the long-term climate simulation to initial vegetation conditions reflects the response of the coupled biosphere-atmosphere system to vegetation perturbations in the case of varying SSTs. Therefore results of the sensitivity experiments shown in Plate 2 can be analyzed in comparison with the multiple climate equilibria (curves A, B, and C) in Plate 1. Comparison between these two Plates shows that the wet regime is, in fact, a reflection of the wet equilibrium A in the scenario of varying SSTs, while the dry regime is a reflection of the dry equilibrium C. The lack of a climate regime that resembles equilibrium B may have to do with the stability of equilibrium B under the influence of varying SSTs. This point is also confirmed by the observation that the climate during the driest period of the wet regime is wetter than equilibrium B, while the climate during the wettest period of the dry regime is drier than equilibrium B. To address this issue, we carry out a group of experiments by restarting the coupled model from

equilibrium B at different times. In Plate 3 the red and green lines show the annual rainfall of these experiments at the grid point near 16°N, while black lines plot the annual rainfall of the wet regime (Dyn-Control) and the dry regime (Dyn-Pert4) for references. LAI and other variables evolve in a similar way. The climate system in the model, although initialized with the medium equilibrium B, eventually converges to either the wet regime or the dry regime depending on when the simulation starts. This suggests that the medium equilibrium B, which is stable under fixed SST forcings, becomes unstable in the scenario of varying SSTs. Only two equilibria (the wet one A and the dry one C) are viable when the interannual variability of SST is included.

5.2. Climate Transitions

It can be observed from Plate 2 that there is no intersection between the wet regime and dry regime, which suggests that the observed SST variability over the Atlantic Ocean alone is not large enough to cause transitions between the two climate regimes, or equivalently, between equilibria A and C. In reality, such transitions may take place due to other large-scale forcings, for example, SST variations over the Pacific and the Indian Oceans which also have a significant impact on the Sahel rainfall [*Palmer*, 1986]. However, due to its zonal symmetry, our model cannot represent the various global-scale forcings. To better understand the behavior of the climate system under the influence of larger external forcings, here we perform two experiments (Wet2 and Dry2) on the system's response to artificially increased SST forcings over the Atlantic Ocean. The Wet2 and Dry2 experiments have the same initial conditions as Dyn-Control and Dyn-Pert4, respectively, but with the magnitude of SST anomalies being doubled (Table 2).

Plate 4 presents the annual rainfall at the grid point near 16°N for Wet2 (green line) and Dry2 (blue line) experiments. Interestingly, Dry2 converges to Wet2 before the end of the decades-long wet event simulated in the early stage of the century. As mentioned in section 5.1, the cold SST in the first several decades of the twentieth century causes a long wet period, which is favorable enough to allow the climate system to develop from an arid equilibrium into a humid one. The impact of this event is obviously enhanced due to the doubling of SST forcings. To avoid this wet event, we start the Dry2 experiment from 1938, 40 years later than 1898. Result of this experiment is also presented in Plate 4 (red line), which introduces a climate regime much drier than the one in Wet2. During most of the time in the 100 years of simulation, climate of the Wet2 experiment is similar to the wet regime explored with observed SST forcings (shown in Plate 2a), which is the reflection of equilibrium A (Plate 1). When starting from 1938, climate of the Dry2 experiment is close to the dry regime and the dry equilibrium C. As demonstrated clearly in Plate 4, climate transitions between different regimes or equilibria take place at various moments. For example, a climate transition from the dry regime to the wet regime is simulated in the early stage of the twenthieth century (around the 1920s), and a reverse transition takes place toward the end of the twenthieth century (in the 1980s). Climate transitions from the wet regime to the dry regime are also triggered around 1934 and 1963, which are interrupted and reversed by subsequent forcings.

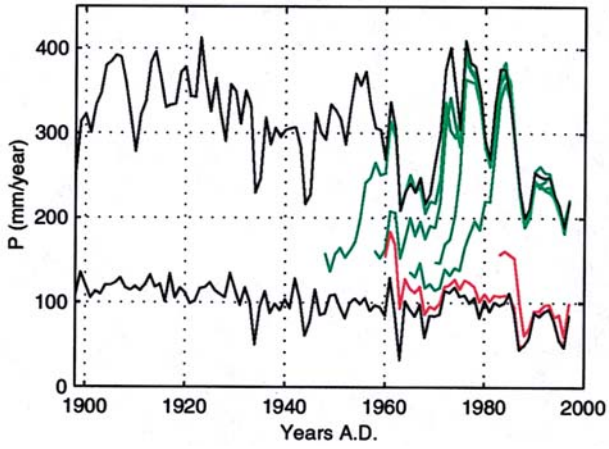

Plate 3. Time series of the annual rainfall at a grid point near 16°N. Green and red lines stand for the experiments that begin from different years with the initial condition at equilibrium B (Plate 1); black lines plot the wet regime (Dyn-Control) and the dry regime (Dyn-Pert4) for references.

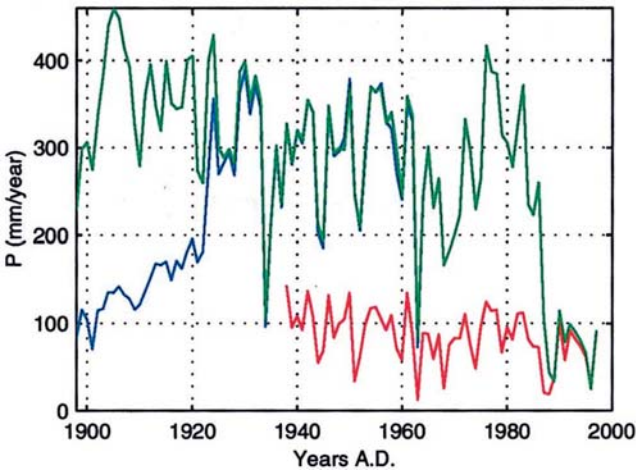

Plate 4. Time series of the annual rainfall at a grid point near 16°N in the Wet2 experiment (green) and the Dry2 experiments starting from 1898 (blue) and 1938 (red).

The Sahel region during several earlier centuries experienced major rainfall fluctuations of large amplitude [*Malay*, 1973, 1981; *Nicholson*, 1981; *Farmer and Wigley*, 1985], which may have to do with transitions of the regional climate system between different equilibria as we demonstrated above. For example, historical lake level records in the Sahel region [e.g., *Farmer and Wigley*, 1985] indicate three major events of rainfall fluctuation since the nineteenth century: a change from wet conditions to dry conditions late in the nineteenth- century, a change from dry conditions to wet conditions early in the twentieth century, and a rapid desiccation later in the twenthieth century. This makes the arid initial condition for 1898 used in Dry2 a better reflection of reality than the initial condition used in Wet2 and Dyn-Control. When starting from 1898, the Dry2 experiment produces a dry episode of almost 2 decades at the beginning of the twentieth century, followed by a climate transition from the dry regime to the wet regime, which agrees well with observations. The rapid climate transition from the wet regime to the dry regime in the 1980s may reflect the occurrence of the current Sahel drought with some time shift.

In summary, the above results strongly suggest the potential for climate transitions between different equilibria or regimes

when the climate system is under the influence of global-scale SST forcings. Climate persistence at one equilibrium and climate transitions between different equilibria collectively compose a special form of climate variability at the timescale of decades to centuries, and therefore can act as another important mechanism contributing to the low-frequency variability of the Sahel rainfall.

6. Discussion and Conclusions

In this paper, based on long-term climate simulations using the coupled biosphere-atmosphere model ZonalBAM, we document two mechanisms for the low-frequency variability of the Sahel rainfall. First, vegetation dynamics enhances the low-frequency variability and suppresses the high-frequency variability of the Sahel rainfall. Large-scale factors including SST variations in the Atlantic Ocean may act as the driving forcing for the climate variability over the Sahel region. However, the response of the regional climate system to these forcings is significantly regulated by vegetation dynamics. Owing to its slow response, vegetation works to amplify and extend the atmospheric anomalies induced by large-scale forcings.

Second, the persistence of the regional climate system at one regime and its transitions between different regimes act as another mechanism that contributes to the low-frequency rainfall variability over the Sahel region. Two climate regimes (wet and dry) have been documented for the regional climate system over West Africa uder the influence of varying SSTs. Large-scale forcings such as changes in the global SST pattern can cause a climate transition from one regime to the other. Such climate transitions, together with the climate persistence at each regime, compose a special type of multidecadal fluctuations or low-frequency variability. It is important to note that vegetation dynamics is a fundamental physical process regulating the climate transitions between different regimes.

The decadal-scale variability in the interhemispheric gradient of global SST, which is statistically related to the low-frequency variability of the Sahel rainfall [*Ward*, 1998], cannot be represented in our zonally symmetric model. However, it is likely that vegetation dynamics could play a significant role in shaping the response of the regional climate system to such global forcings.

Our experiments on the model's sensitivity to initial conditions are of a similar nature to ensemble simulations frequently used in weather forecasting studies [e.g., *Buizza and Palmer*, 1998]. Ensemble simulations are designed to address the uncertainty associated with atmospheric chaos. In reality, the persistence of chaos-induced anomalies, provided by the two-way biosphere-atmosphere feedback, may contribute to the interannual variability of the regional climate. However, there is a very good convergence between different simulations within one climate regime of our model (e.g., Plates 2 and 3), which may suggest that the year-to-year climate variability associated with atmospheric chaos is negligible in the context of this model. The weakness of the chaos-induced interannual variability might be another potential factor, in addition to those cited in section 4.1, that contributes to the differences between the model simulation and observations (Figure 3a versus Figure 4).

In this study we focus on the natural biosphere-atmosphere system without considering the impact of human activities which have effectively reshaped the West African landscape [e.g., *Bourliere and Hadley*, 1983 *Fairhead and Leach*, 1998]. Therefore the vegetation variation simulated in this study is not comparable with observations [e.g., *Myneni et al*., 1998] which results from both natural processes and human-induced disturbances. Because of the same reason, the variability of the simulated climate is not comparable with observations either, as already discussed in section 4. Further research on how the human land use in the past several decades may have altered the coupled biosphere-atmosphere system is underway.

Acknowledgments. We thank Ignacio Rodriguez-Iturbe for discussion and suggestions. We also thank the anonymous reviewers for their helpful comments. NCEP reanalysis data were provided by the NOAA-CIRES Climate Diagnostics Center, Boulder, Colorado. GPCP data were provided by the World Data Centre for Meteorology, NCDC, Asheville, North Carolina. This research has been supported by the National Aeronautics and Space Administration (NASA) under agreement NAGW-5201, NAG5-7525, and NAG5-8617, and by the National Science Foundation (NSF) under agreement ATM 9807068. The views, opinions, and/or findings contained in this paper are those of the authors and should not be construed as an official NASA, or NSF, position, policy, or decision, unless so designated by other documentation.

References

Bourliere, F., and M. Hadley, Present-day savannas: An overview, in *Ecosystem of the World—Tropical Savannas*, edited by F. Bourliere, pp. 1–17, Elsevier Sci., New York, 1983.

Buizza, R., and T. N. Palmer, Impact of ensemble size on ensemble prediction, *Mon. Weather Rev*., *126*, 2503–2518, 1998.

Charney, J., W. J. Quirk, S. Chow, and J. Kornfield, A comparative study of the effects of albedo change on drought in semi-arid regions, *J. Atmos. Sci*., *34*, 1366–1385, 1977.

Dansgaard, W., S. J. Johnsen, N. Reeh, N. Gundestrup, H. B. Clausen, and C. U. Hammer, Climatic changes, Norsemen and modern man, *Nature*, *255*, 24–28, 1975.

Demaree, G. R., and C. Nicolis, Onset of Sahelian drought viewed as a fluctuation-induced transition, *Q. J. R. Meteorol. Soc*., *116*, 221–238, 1990.

Entekhabi, D., I. Rodriguez-Iturbe, and R. Bras, Variability in large-scale water balance with land surface-atmosphere interaction, *J. Clim*., *5*, 798–813, 1992.

Fairhead, J., and M. Leach, Reconsidering the extent of deforestation in twentieth century West Africa, *Unasylva*, *192*(49), 38–46, 1998.

Farmer, G., and T. M. L. Wigley, Climatic trends for tropical Africa, research report, 136 pp., Univ. of East Anglia, Norwich, England, 1985.

Foley, J. A., I. C. Prentice, N. Ramankutty, S. Levis, D. Pollard, S. Sitch, and A. Haxeltine, An integrated biosphere model of land surface processes, terrestrial carbon balance, and vegetation dynamics, *Global Biogeochem. Cycles*, *10*, 603–628, 1996.

Folland, C., J. Owen, M. N. Ward, and A. Colman, Prediction of seasonal rainfall in the Sahel region using empirical and dynamical methods, *J. Forecasting*, *10*, 21–56, 1991.

Gornitz, V., and NASA, A survey of anthropogenic vegetation changes in West Africa during the last century—Climatic implications, *Clim. Change*, *7*, 285–325, 1985.

Hastenrath, S. L., Interannual variability and annual cycle: Mechanisms of circulation and climate in the tropical Atlantic sector, *Mon. Weather Rev*., *112*, 1097–1107, 1984.

Hulme, M., T. J. Osborn, and T. C. Johns, Precipitation sensitivity to global warming: Comparison of observations with HadCM2 simulations, *Geophys. Res. Lett*, *25*, 3379–3382, 1998.

Kalnay, E., et al., The NCEP/NCAR 40-year reanalysis project, *Bull. Am. Meteorol. Soc.*, *77*, 437–471, 1996.

Lamb, P. J., Case studies of tropical Atlantic surface circulation patterns during recent sub-Saharan weather anomalies: 1967 and 1968, *Mon. Weather Rev*., *106*, 482–491, 1978a.

Lamb, P. J., Large-scale tropical Atlantic surface circulation patterns associated with sub-Saharan weather anomalies, *Tellus*, *30*, 240–251, 1978b.

Lough, J. M., Tropical Atlantic sea-surface temperatures and rainfall

variations in sub-Saharan Africa, *Mon. Weather Rev*., *114*, 561–570, 1986.
Maley, J., Mecanisme des changements climatiques aux basses latitudes, *Palaeogeogr. Palaeoclimatol. Palaeoecol*., *14*, 193–227, 1973.
Maley, J., Etudes palynologiques dans le bassin du Tchad et pal'eoclimatologie de l'Afrique nord-tropicale de 30,000 ans a l'epoque actuelle, *Tech. Rep*. *129*, Inst. Fr. de Rech. Sci. pour le Dev. en Coop. (ORSTOM), Paris, France, 1981.
Menaut, J.-C., The vegetation of African savannas, in *Ecosystem of the World—Tropical Savannas*, edited by F. Bourliere, pp. 109–142, Elsevier Sci., New York, 1983.
Myneni, R. B., C. J. Tucker, G. Asrar, and C. D. Keeling, Interannual variations in satellite-sensed vegetation index data from 1981 to 1991, *J. Geophys. Res*., *103*, 6145–6160, 1998.
Nicholson, S. E., The historical climatology of Africa, in *Climate and History*, edited by T. M. L. Wigley, M. J. Ingram, and G. Farmer, pp. 249–270, Cambridge Univ. Press, New York, 1981.
Nicholson, S. E., African drought: Characteristics, causal theories and global teleconnections, *Geophys. Monogr*., *52*(7), 79–100, 1989.
Nicholson, S. E., and D. Entekhabi, The quasi-periodic behavior of rainfall variability in Africa and its relationship to the Southern Oscillation, *Rach. Meteorol. Geophys. Bioclim., Ser. A*, *34*, 311–348, 1986.
Nicholson, S. E., and I. M. Palao, A re-evaluation of rainfall variability in the Sahel, part I, Characteristics of rainfall fluctuations, *Int. J. Climatol*., *13*, 371–389, 1993.
Nicolis, C., Stochastic aspects of climate transitions—Response to a periodic forcing, *Tellus*, *34*, 1–9, 1982.
Palmer, T. N., The influence of the Atlantic, Pacific, and Indian Oceans on Sahel rainfall, *Nature*, *322*, 251–253, 1986.
Parker, D. E., M. Jackson, and E. B. Horton, The GISST2.2 Sea Surface Temperature and Sea-Ice Climatology, *Clim. Res. Tech. Note 63 (CRTN63)*, U.K. Meteorol. Off., Bracknell, Berkshire, England, 1985.
Porter, S. C., Pattern and forcing of northern hemisphere glacier variations during the last millenium, *Quat. Res*., *26*, 27–48, 1986.
Rayner, N. A., E. B. Horton, D. E. Parker, C. K. Folland, and R. B. Hackett, Version 2.2 of the Global Sea-Ice and Sea Surface Temperature data set, 1903–1994, *Clim. Res. Tech. Note 74 (CRTN74)*, U.K. Meteorol. Off., Bracknell, Berkshire, England, 1996.
Rodriguez-Iturbe, I., D. Entekhabi, and R. L. Bras, Nonlinear dynamics of soil moisture at climate scales, 1, Stochastic analysis, *Water Resour. Res*., *27*, 1899–1906, 1991.
Rowell, D. P., C. K. Folland, K. Maskell, and M. N. Ward, Variability of summer rainfall over tropical North Africa (1906–92): Observations and modeling, *Q. J. R. Meteorol. Soc*., *121*, 669–704, 1995.
Shukla, J., Predictability in the midst of chaos: A scientific basis for climate forecasting, *Science*, *282*, 728–731, 1998.
Sud, Y. C., and A. Molod, A GCM simulation study of the influence of Saharan evapotranspiration and surface-albedo anomalies on July circulation and rainfall, *Mon. Weather Rev*., *116*, 2388–2400, 1988.
Wang, G., and E. A. B. Eltahir, Biosphere-atmosphere interactions over West Africa, 1, Development and validation of a coupled dynamic model, *Q. J. R. Meteorol. Soc*., in press, 1999a.
Wang, G., and E. A. B. Eltahir, Biosphere-atmosphere interactions over West Africa, 2, Multiple climate equilibria, *Q. J. R. Meteorol. Soc*., in press, 1999b.
Wang, G., and E. A. B. Eltahir, Impact of rainfall sub-grid variability on modeling the biosphere-atmosphere system, *J. Clim*., in press, 1999c.
Ward, M. N., Diagnosis and short-lead time prediction of summer rainfall in tropical North Africa at interannual and multidecadal timescales, *J. Clim*., *11*, 3167–3191, 1998.
Xue, Y., Biosphere feedback on regional climate in tropical North Africa, *Q. J. R. Meteorol. Soc*., *123*, 1483–1515, 1997.
Xue, Y., and J. Shukla, The influence of land surface properties on Sahel climate, Part I, Desertification, *J. Clim*., *6*, 2232–2245, 1993.
Zhang, H., and A. Henderson-Sellers, Impacts of tropical deforestation, part I, Process analysis of local climate change, *J. Clim*., *9*, 1497–1517, 1996.
Zheng, X., and E. A. B. Eltahir, The response to deforestation and desertification in a model of West African monsoons, *Geophys. Res. Lett*., *24*, 155–158, 1997.
Zheng, X., and E. A. B. Eltahir, The role of vegetation in the dynamics of West African monsoons, *J. Clim*., *11*, 2078–2096, 1998.
Zheng, X., E. A. B. Eltahir, and K. A. Emanuel, A mechanism relating tropical Atlantic spring sea surface temperature and west African rainfall, *Q. J. R. Meteorol. Soc*., *125*, 1129–1164, 1999.

E. A. B. Eltahir and G. Wang, Ralph M. Parsons Laboratory, Department of Civil and Environmental Engineering, MIT, Cambridge, MA 02139.

(Received July 20, 1999; revised December 13, 1999;
accepted December 27, 1999.)